PAPER

Hybrid Model for Cascading Outage in a Power System: A Numerical Study*

Yoshihiko SUSUKI[†a)], ***Member***, **Yu TAKATSUJI**[†b)], ***Student Member***, ***and*** **Takashi HIKIHARA**[†c)], ***Member***

SUMMARY Analysis of cascading outages in power systems is important for understanding why large blackouts emerge and how to prevent them. Cascading outages are complex dynamics of power systems, and one cause of them is the interaction between swing dynamics of synchronous machines and protection operation of relays and circuit breakers. This paper uses hybrid dynamical systems as a mathematical model for cascading outages caused by the interaction. Hybrid dynamical systems can combine families of flows describing swing dynamics with switching rules that are based on protection operation. This paper refers to data on a cascading outage in the September 2003 blackout in Italy and shows a hybrid dynamical system by which propagation of outages reproduced is consistent with the data. This result suggests that hybrid dynamical systems can provide an effective model for the analysis of cascading outages in power systems.

key words: *power system, cascading outage, modeling, hybrid dynamical system*

1. Introduction

Complex dynamics have recently emerged as a major issue in electric power systems [1], [2]. Various technological advances and economic reform are known in power system engineering. Examples include development of semiconductor-based power apparatuses, penetration of distributed power sources, and deregulation of power markets. It is widely expected that these advances lead to a robust infrastructure for electricity supply. On the other hand, they make it difficult to grasp and tame dynamics of power systems and possibly cause the dynamics to be unpredictable. Cascading outage is one important example of the dynamics and is the generic mechanism by which outages propagate to cause widespread blackouts of power systems [3], for example, the August 2003 blackout in North America [4].

Transient stability of power systems is closely related to the occurrence of cascading outages. Transient stability is concerned with the ability of power system to maintain synchronism when subjected to a severe disturbance [5], [6]. The stability is mainly governed by swing dynamics of synchronous machines. A swing usually causes overcurrents and heavy power flows. This often results in the outages of transmission and generation facilities by relay operation to protect them. They can cause further swings, thereby inducing the outages of other facilities. The interaction between swing dynamics governing transient stability and protection operation is observed in cascading outages of real power systems, for example, the September 2003 blackout in Italy [4], [7]. As indicated by [8]–[10], the interaction involves hybrid modeling, implying that it is modeled with both continuous- and discrete-valued variables.

Extensive studies have been devoted to modeling of cascading outages in power systems. Dobson et al. [3] proposed probabilistic models for cascading outages. Kinney et al. [11] used a simple graph-based model for the analysis of North American power grid. They revealed statistical features of cascading outages. Parrilo et al. [12] and DeMarco [13] analyzed dynamic features of cascading outages using classical models of transient stability. Accurate mathematical models are used in power system analyzers such as EMTP and RTDS that can simulate cascading outages in detail. These models are often specific to particular systems and do not readily reveal dynamical principles, because the models are not amenable to analytical comparative studies. Then it needs to seek a balance between such complexity and simpler phenomenological models.

We develop and analyze a mathematical model of cascading outage in a power system. Following the importance of transient stability, this paper focuses on the interaction between swing dynamics and protection operation. The developed model is a hybrid dynamical system [14]–[16] and consists of families of flows describing swing dynamics and their switching rules that are based on control schemes of protection operation. The model also can be formulated as hybrid automaton [17] which is introduced to model power systems by Hiskens [18], Fourlas et al. [19], and Hikihara et al. [20], [21]. This paper refers to data on a cascading outage in the September 2003 blackout in Italy [7] and shows a hybrid dynamical model by which propagation of outages reproduced is consistent with the data. Numerical simulations of the hybrid dynamical system also show that control schemes of protection operation affect the occurrence of the cascading outage. Preliminary discussions of this paper are in [22], [23].

This paper is organized as follows: Sect. 2 reviews data observed in a cascading outage in the September 2003 blackout in Italy [7]. Section 3 reviews a continuous-time model for swing dynamics [24], [25] and control schemes of overcurrent relay and circuit breaker [26], thereby deriv-

Manuscript received June 11, 2008.
Manuscript revised October 2, 2008.

[†]The authors are with Department of Electrical Engineering, Kyoto University, Kyoto-shi, 615-8510 Japan.

*This research is supported in part by the Ministry of Education, Culture, Sports, Sciences and Technology in Japan, The 21st Century COE Program #14213201 and Young Research (B) #18760216, 2007.

a) E-mail: susuki@dove.kuee.kyoto-u.ac.jp
b) E-mail: takatsuji@dove.kuee.kyoto-u.ac.jp
c) E-mail: hikihara@kuee.kyoto-u.ac.jp

DOI: 10.1587/transfun.E92.A.871

ing a hybrid dynamical system as a mathematical model of the cascading outage. Section 4 performs numerical simulations of the hybrid dynamical system. Section 5 is the conclusion of this paper with a summary and future work.

2. Cascading Outage in the September 2003 Blackout in Italy

Before modeling in Sects. 3 and 4, this section reviews data observed in a cascading outage in the September 2003 Blackout in Italy. This review is based on [7]. The Italian power system experienced a large blackout on September 28, 2003. The blackout affected an area with an estimated 60 million people and load variation in the continental grid from about 24000 MW at the early hours of the day, up to 50000 MW in the mid-day. This is regarded as the largest blackout ever to happen in Italy.

Figure 1 shows (a) 400 kV and (b) 220 kV power transmission networks interconnecting Italy with France and Switzerland. A cascading outage or trip of transmission lines is indicated according to the time they tripped, starting from #1 at 3:01.42 up to #9 at 3:25.33. The cascading trip resulted in the separation of Italian network from Switzerland and French ones and, after further cascading trips of generators in Italy, finally led to the blackout.

Figure 1(c) shows frequency traces on three EHV (Extra High Voltage) substations from 3:25.12 up to 3:26.12. Three pulsing behaviors are observed in Fig. 1(c) during the period from line trip #2 at 3:25.21 up to #5 at 3:25.27. It is indicated in [7] that the observed behaviors are caused by the interaction between transient stability governed by swing dynamics and protection operation. The swing dynamics cause heavy power flows that trigger the protection operation. The operation is normally based on overcurrent or distance relaying. This paper investigates the swing dynamics related to the cascading trip of transmission lines.

It should be noted that various frequency dynamics are observed in Fig. 1(c). For example, the line trip # 8 at 3:25.33 in Figs. 1(a) and (b) triggered continuous decrease of frequency below 48.5 Hz in Fig. 1(c). The associated dynamics result in the isolation of Italian network and the blackout. Here, from a phenomenological point of view, they are modeled through an interacting system with swing dynamics, voltage dynamics, and protection operation. However, this modeling and analytical studies are not easy. As the first step of analytical studies on cascading outage, this paper focuses on the relatively simple cascading outage, and the detailed modeling is in future work as mentioned in Sect. 5.

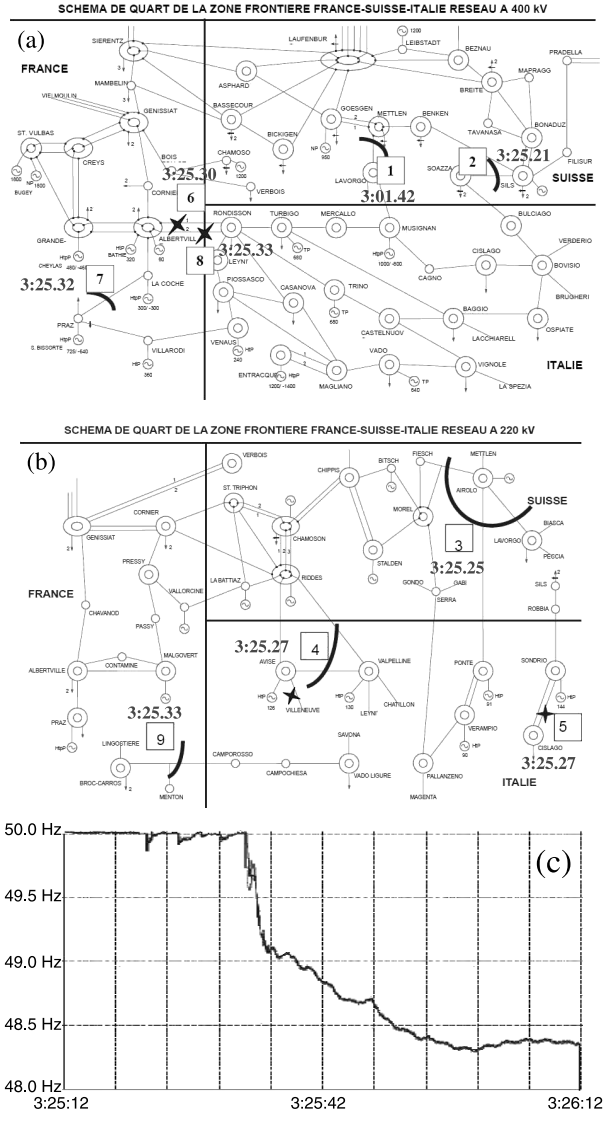

Fig. 1 Data of the September 2003 Blackout in Italy. (a) and (b) are Fig. 2 in [7] and show (a) 400 kV and (b) 220 kV power transmission networks interconnecting Italy with France and Switzerland. They indicate the propagation of line trips (outages) according to the time they tripped, starting from #1 at 3:01.42 up to #9 at 3:25.33. (c) is Fig. 4 in [7] and shows frequency traces in North Italy at Piossasco, S. Rocco, and Musignano EHV substations from 3:25.12 up to 3:26.12. Adapted and reprinted with permission from [7] ©2004 IEEE.

3. Hybrid Model for the Cascading Outage

This section derives a hybrid dynamical system as a mathematical model of the cascading outage in Sect. 2. Section 3.1 gives the six-machine power system model by which we consider the cascading outage in this paper. Section 3.2 reviews a classical model for swing dynamics of synchronous machines [24], [25] that describe a family of flows. Section 3.3 reviews control schemes of overcurrent relays and circuit breakers [26] that are modeled as switching rules of flows. Section 3.4 integrates the continuous-time model with the switching rules and provides a hybrid dynamical system for the cascading outage.

3.1 Six-Machine Power System Model

Figure 2 shows the six-machine power system model. The interconnected power system in Figs. 1(a) and (b) is decomposed into several subsystems that are represented by equivalent synchronous machines and constant power loads. Note

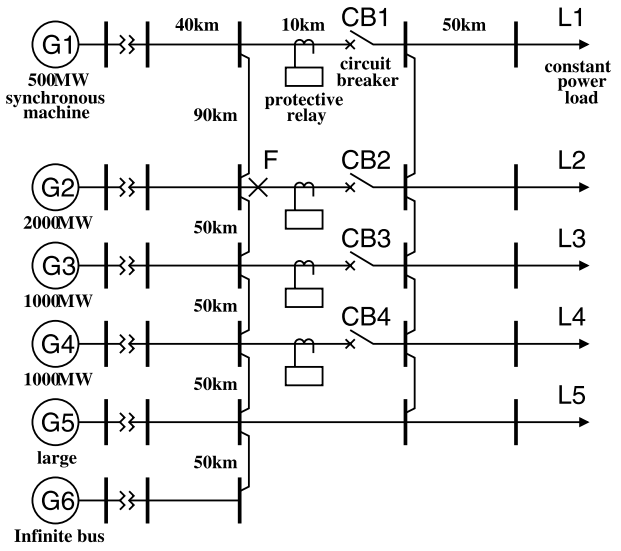

Fig. 2 Six-machine power system model that is based on Figs. 1(a) and (b). The six equivalent machines G1–G6 represent the Switzerland and French power systems, and the loads, denoted by the right-arrows, represent the Italian power system. G6 is assumed to be the infinite bus [5]. The transmission lines with protective overcurrent relays and circuit breakers CB1–CB4 connect the Italian system with others. CB1 is related to the line trip #5 in Fig. 1(b), CB2 to #2 in Fig. 1(a), CB3 to #3 in Fig. 1(b), and CB4 to #4 in Fig. 1(b).

that the decomposition is not unique and depends on modeling purpose. The six equivalent machines G1–G6 represent the Switzerland and French power systems, and the loads, denoted by the arrows, represent the Italian power system. The direction of power flows is hence from the Switzerland and French power systems to the Italian one. This is consistent with the data [7]. G6 is assumed to be the infinite bus [5]. The transmission lines with overcurrent relays and circuit breakers CB1–CB4 connect the Italian system with others. CB1 is related to the line trip #5 in Fig. 1(b), CB2 to #2 in Fig. 1(a), CB3 to #3 in Fig. 1(b), and CB4 to #4 in Fig. 1(b). Hence the propagation of line trips in the data is CB2 → CB3 → CB4 → CB1 under swing dynamics of G1–G5 in Fig. 2. The following subsections treat the interaction between swing dynamics and protection operation in Fig. 2.

3.2 Continuous-Time Model for Swing Dynamics

We use the so-called classical model [24], [25] of swing dynamics of synchronous machines. The classical model describes swing dynamics of machine Gi ($i = 1, \ldots, 5$) by the following ordinary differential equations:

$$\left.\begin{aligned} \dot{\delta}_i &= \omega_i, \\ \frac{P_{ri}}{P_b}\frac{H_i}{\pi f_s}\dot{\omega}_i &= p_{mi} - d_i\omega_i - p_{ei}(\delta_1, \ldots, \delta_6). \end{aligned}\right\} \quad (1)$$

$\dot{x}$ is the time (t) differentiation of variable x. δ_i is the rotor angle position of Gi with respect to the infinite bus G6, ω_i the rotor speed deviation of Gi relative to system angular frequency $2\pi f_s$. δ_6 for G6 is assumed to be zero. P_b, P_{ri}, H_i, f_s, p_{mi}, and d_i are parameters of the classical model (1). P_b is the base power in per unit system. P_{ri} is the rated power of Gi, H_i its per-unit inertia constant, p_{mi} the mechanical input power to Gi, and d_i its damping coefficient. p_{ei} stands for the electrical output power of Gi and is given by the following function of all rotor angle positions $\delta_1, \ldots, \delta_6$:

$$p_{ei} \triangleq G_{ii}E_i^2 + \sum_{j=1, j\neq i}^{6} E_iE_j\left\{G_{ij}\cos(\delta_i - \delta_j) + B_{ij}\sin(\delta_i - \delta_j)\right\}. \quad (2)$$

E_i is the terminal voltage of Gi, G_{ii} its internal conductance, and $G_{ij} + \mathrm{j}B_{ij}$ the transfer admittance between Gi and Gj. Note that the loads in Fig. 2 are modeled as passive impedances [25]. E_i, G_{ii}, G_{ij}, and B_{ij} are other parameters and can be determined with power flow calculation.

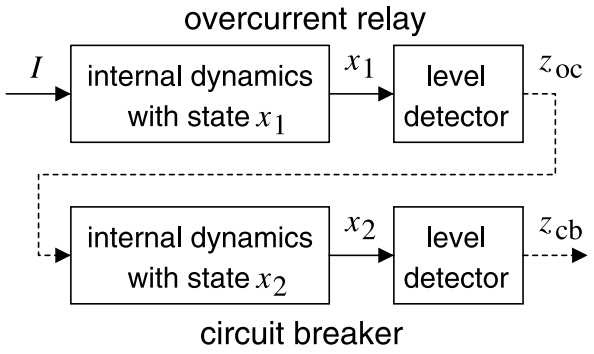

Fig. 3 Control scheme diagram of overcurrent relay and circuit breaker showing operation of induction-disc type overcurrent relay and circuit breaker [26]. The solid arrows denote continuous signals, and the broken arrows discrete ones. The relay and breaker have internal dynamics represented by ordinary differential equations of x_1 and x_2. Level detector produces the discrete outputs $z_{oc}, z_{cb} \in \{0, 1\}$ that are determined by whether the states x_1 and x_2 are greater than prescribed thresholds or not.

3.3 Control Schemes of Protection Operation

We next describe control schemes of protection operation in overcurrent relays and circuit breakers. Perez et al. [26] modeled protective relay systems for power system dynamics analysis. Our modeling relies on their mathematical models of relay operation.

Figure 3 shows control sequences of overcurrent relay and circuit breaker with internal dynamics. I is the input of line current and is a function of rotor angle positions $\delta_1, \ldots, \delta_6$. The internal dynamics are described by differential equations of state variables x_1 for relay and x_2 for circuit breaker. Level detector produces the discrete output 1 (or 0) when the magnitude of input is greater (or less) than a prescribed threshold. z_{oc} and z_{cb} in Fig. 3 denote the discrete outputs of the overcurrent relay and the circuit breaker. The condition $z_{cb} = 1$ is associated with that when the corresponding circuit breaker opens, in other words, the line is disconnected; $z_{cb} = 0$ when it closes. Thus the output z_{cb} determines the condition of transmission lines and regulates the network topology of six-machine power system model.

The internal dynamics and level detector of induction-disc type overcurrent relay are described in [26] as

$$\left.\begin{aligned} \dot{x}_1 &= g(I)\{1 - \nu(x_1 - x_{\mathrm{TDS}})\nu(I - I_{\mathrm{TAP}})\}, \\ z_{\mathrm{oc}} &= \nu(x_1 - x_{\mathrm{TDS}}), \end{aligned}\right\} \tag{3}$$

where

$$\left.\begin{aligned} g(I) &\triangleq K\left\{\left(\frac{I}{I_{\mathrm{TAP}}}\right)^2 - 1\right\}, \\ \nu(x) &\triangleq \begin{cases} 0 & \text{if } x \le 0, \\ 1 & \text{if } x > 0. \end{cases} \end{aligned}\right\} \tag{4}$$

The level detector in Fig. 3 is defined as the step function ν of state x_1. I_{TAP}, x_{TDS}, and K are the tuning parameters of overcurrent relay and are assumed to be constant. I_{TAP} is the prescribed threshold value of input current I, x_{TDS} the threshold value of state x_1, and K the acceleration factor of internal dynamics. On the other hand, the internal dynamics and level detector of circuit breaker are described in [26] as

$$\left.\begin{aligned} \tau\dot{x}_2 &= z_{\mathrm{oc}}\{1 - \nu(x_2 - x_{\mathrm{tr}})\}, \\ z_{\mathrm{cb}} &= \nu(x_2 - x_{\mathrm{tr}}). \end{aligned}\right\} \tag{5}$$

The parameters x_{tr} and τ for operation of the circuit breaker are also assumed to be constant. x_{tr} is the threshold value of x_2, and τ the time constant for internal dynamics.

3.4 Hybrid Dynamical System

By combining the continuous-time model for swing dynamics in Sect. 3.2 with the control schemes of protection operation in Sect. 3.3, we can derive a hybrid dynamical system as a mathematical model for the cascading outage. A definition of hybrid dynamical systems is given in [14]–[16].

First, all candidates of network topologies of the six-machine power system model are described using a finite index set. This section aims to model the interaction between swing dynamics of G1–G5 and line trips of CB1–CB4. The parameters G_{ii}, G_{ij}, and B_{ij} in the classical model (1) discontinuously change when the circuit breakers disconnect the lines. Then it needs to describe all candidates of network topologies explicitly. Let us define a finite index set Q as

$$\begin{aligned} Q \triangleq \{&1234, 123, 124, 134, 234, \\ &12, 13, 14, 23, 24, 34, 1, 2, 3, 4, 0\}. \end{aligned} \tag{6}$$

The index $1234 \in Q$ denotes the network topology under no trip of CB1–CB4, 123 under trip of CB4, 0 under all trips of CB1–CB4, and so on.

Second, the swing dynamics of G1–G5 are described using a family of flows. To do so, we re-write the classical model (1) that makes it possible to take the network topologies into account. The electrical output $p_{\mathrm{e}i}^{(\alpha)}$ indexed by $\alpha \in Q$ that describes one network topology is given by

$$\begin{aligned} p_{\mathrm{e}i}^{(\alpha)} = G_{ii}^{(\alpha)}E_i^2 + \sum_{j=1, j\neq i}^{6} E_iE_j\Big\{&G_{ij}^{(\alpha)}\cos(\delta_i - \delta_j) \\ &+ B_{ij}^{(\alpha)}\sin(\delta_i - \delta_j)\Big\}. \end{aligned} \tag{7}$$

The parameter $G_{ii}^{(\alpha)}$ denotes the internal impedance of Gi for index α, and similarly for $G_{ij}^{(\alpha)}$ and $B_{ij}^{(\alpha)}$. Here V_α denotes an open subspace of $S^5 \times \mathbb{R}^5$ whose elements are the rotor angle positions $\delta_1, \ldots, \delta_5$ and rotor speed deviation $\omega_1, \ldots, \omega_5$. The subspace is called chart [14], [16]. The collection of charts, $V = \bigcup_{\alpha\in Q} V_\alpha$, is also called atlas [14], [16]. Each chart is associated with a flow $f_\alpha : V_\alpha \to \mathbb{R}^{10}$, defined by the classical model (1) indexed by $\alpha \in Q$. Thus the swing dynamics of G1–G5 are described by a family of flows, $\{f_\alpha\}_{\alpha\in Q}$, defined on the atlas V.

Third, the control schemes of protection operation are described using switching between flows. Consider the control schemes in Sect. 3.3. V_{c} denotes an open subspace of $\mathbb{R}^8$ whose elements are the internal states $(x_{11}, x_{21}, \ldots, x_{14}, x_{24})^{\mathrm{T}}$. The variables (x_{1i}, x_{2i}) represent the states for CBi. Eqs. (3) and (5) define a flow $f_{\mathrm{c}} : V_\alpha \times V_{\mathrm{c}} \to \mathbb{R}^8$. The reason that V_α is here contained in the definition of f_{c} is that Eq. (3) has the input current I which is a function of rotor angle positions $(\delta_1, \ldots, \delta_5) \in V_\alpha$. Then, by referring to [16], for each $\alpha \in Q$ we have a collection of functions $h_\alpha^\beta : V_\alpha \times V_{\mathrm{c}} \to \{0, 1\}$ indexed by β. As points flow across a chart, the threshold functions h_α^β monitor whether a transition to a (possibly) new chart should occur at that instant. When the function h_α^β becomes unity, the trajectory switches to a chart described by the index β. The concrete description of h_α^β is given by the discrete outputs $z_{\mathrm{cb}1}, \ldots, z_{\mathrm{cb}4}$ in Eq. (5). Switching between charts occurs via mappings $\mathcal{T}_\alpha^\beta$ with domains in V_α and ranges in V_β. It is assumed in our modeling that there is no reset of variables, in other words, $\mathcal{T}_\alpha^\beta$ is the identity mapping.

Thus, we can describe the interaction between swing dynamics and protection operation using a hybrid dynamical system as the following collection H:

$$\mathsf{H} = (Q, V_\alpha, f_\alpha, h_\alpha^\beta, \mathcal{T}_\alpha^\beta, V_{\mathrm{c}}, f_{\mathrm{c}}). \tag{8}$$

Here it is worth mentioning that H is re-formulated as a hybrid automaton [17], [27]. Q is the set of finite discrete states, and $V_\alpha \times V_{\mathrm{c}}$ the set of continuous states. f_α and f_{c} represent the continuous dynamics (vectorfields) defined by Eqs. (1), (3) and (5), and $\mathcal{T}_\alpha^\beta$ the reset function [27] or, in our modeling, mapping between different discrete states. h_α^β is regarded as a guard condition [27] for discrete evolution that determines whether mapping $\mathcal{T}_\alpha^\beta$ should occur. Hence verification algorithms and tools for hybrid automaton are applicable to our hybrid model for the cascading outage.

4. Analysis of the Cascading Outage

This section analyzes the hybrid dynamical system H. Table 1 shows the configuration and parameter setting in six-machine power system model that are used for numerical simulations. They are based on the data [7]. It is supposed that there is no control equipment of synchronous machines such as AVR (Automatic Voltage Regulator) and PSS

Table 1 Configuration and parameter setting of six-machine power system model.

VA base P_b		2000 MW
Voltage base		400 kV
System frequency f_s		50 Hz
Machine rating $P_{\mathrm{r}i}$ of Gi	$i = 1$	500 MW
	$i = 2$	2000 MW
	$i = 3, 4$	1000 MW
	$i = 5$	200 GW
Per-unit inertia constant H_i of Gi	$i = 1, \ldots, 5$	5 s
Damping coefficient d_i of Gi	$i = 1, \ldots, 5$	0.05
Mechanical input power $p_{\mathrm{m}i}$ to Gi	$i = 1$	0.2
	$i = 2$	0.95
	$i = 3$	0.45
	$i = 4$	0.35
	$i = 5$	1.25
Terminal voltage E_i of Gi	$i = 1, \ldots, 5$	1
Line inductance of π-equivalent circuit model		0.9 mH/km
Line resistance		0 Ω/km
Line capacitance		0 F/km
Transformer impedance		0.15
Constant active power flow to load Li	$i = 1$	0.2
	$i = 2$	0.95
	$i = 3$	0.45
	$i = 4$	0.35
	$i = 5$	1.25
Constant reactive power flow to load Li	$i = 1, \ldots, 5$	0
Parameters of overcurrent relay	I_TAP	1.03
	K	16
	x_TDS	1
circuit breaker	τ	0.1 s
	x_tr	1

(Power System Stabilizer), and that there is also no LRT (Load Ratio control Transformer) with machine buses. This section shows that the hybrid dynamical system reproduces the propagation of outages in Fig. 1 and provides dynamical features of the propagation.

4.1 Numerical Experiment

This section performs numerical simulations for swing dynamics and protection operation in six-machine power system model. The bus voltages are fixed through power flow calculation. Steady state conditions of rotor angle position δ_i ($i = 1, \ldots, 5$) are also determined through the calculation and are used as the initial condition $\delta_i(t = 0\,\mathrm{s})$. By putting the initial condition $\omega_i(0\,\mathrm{s}) = 0$ ($i = 1, \ldots, 5$), it is possible to start numerical simulations from the steady state conditions. The initial conditions of internal states (x_{1i}, x_{2i}) ($i = 1, \ldots, 4$) are also fixed at $(x_{1i}(0\,\mathrm{s}), x_{2i}(0\,\mathrm{s})) = (0, 0)$. The parameters $G_{ii}^{(\alpha)}$, $G_{ij}^{(\alpha)}$, and $B_{ij}^{(\alpha)}$ for each $\alpha \in Q$ are also determined through the power flow calculation. It is here supposed that each machine is in the steady state condition at $t < 0\,\mathrm{s}$, that a three-phase fault occurs at point F near G2 bus at $t = 0\,\mathrm{s}$, and that the fault is removed at $t = t_\mathrm{c}$. t_c corresponds to the fault duration.

Figure 4 shows time responses of rotor angle position δ_i, rotor speed deviation ω_i, internal states (x_{1i}, x_{2i}) and discrete outputs $(z_{\mathrm{oc}i}, z_{\mathrm{cb}i})$ for protection operation. The figure is for fault duration $t_\mathrm{c} = 0.112\,\mathrm{s} \approx 5.6$ cycles of a 50-Hz sine wave. A cascade of line trips is observed:

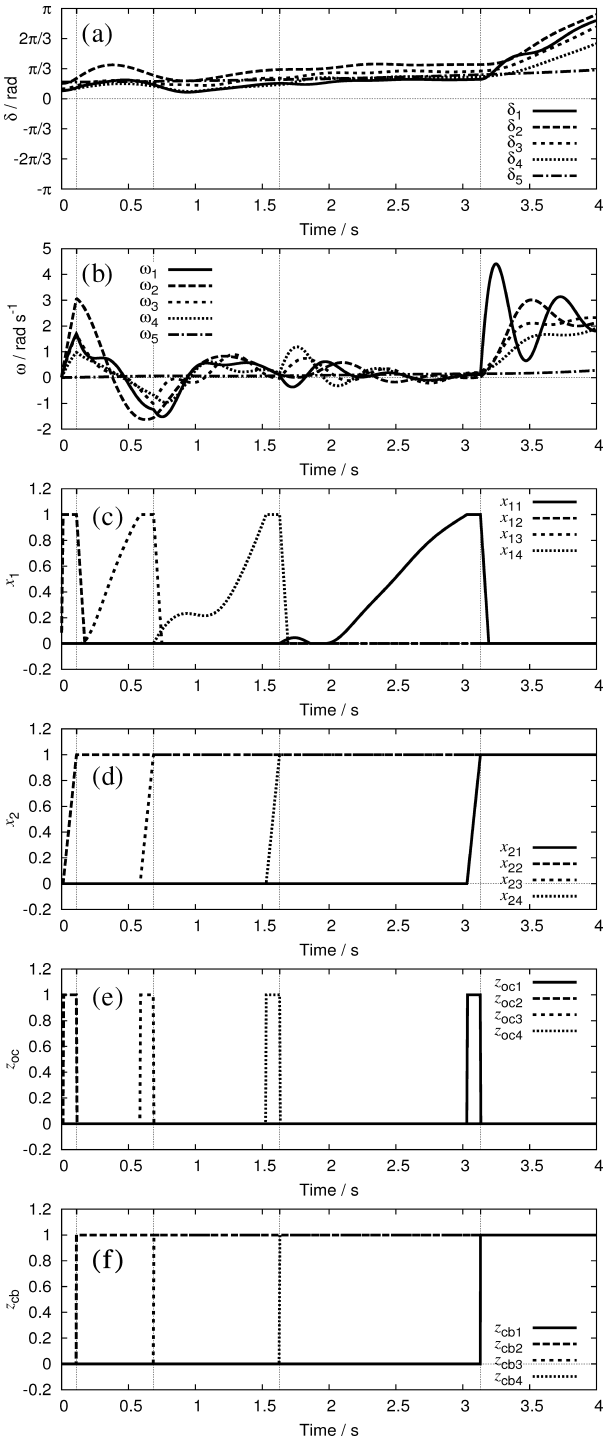

Fig. 4 Swing dynamics and protection operation in six-machine power system model. (a) Rotor angle position δ_i; (b) Rotor speed deviation ω_i; (c) internal state x_{1i} of overcurrent relays; (d) internal state x_{2i} of circuit breakers; (e) discrete output $x_{\mathrm{oc}i}$ of overcurrent relays; (f) discrete output $z_{\mathrm{cb}i}$ of circuit breakers.

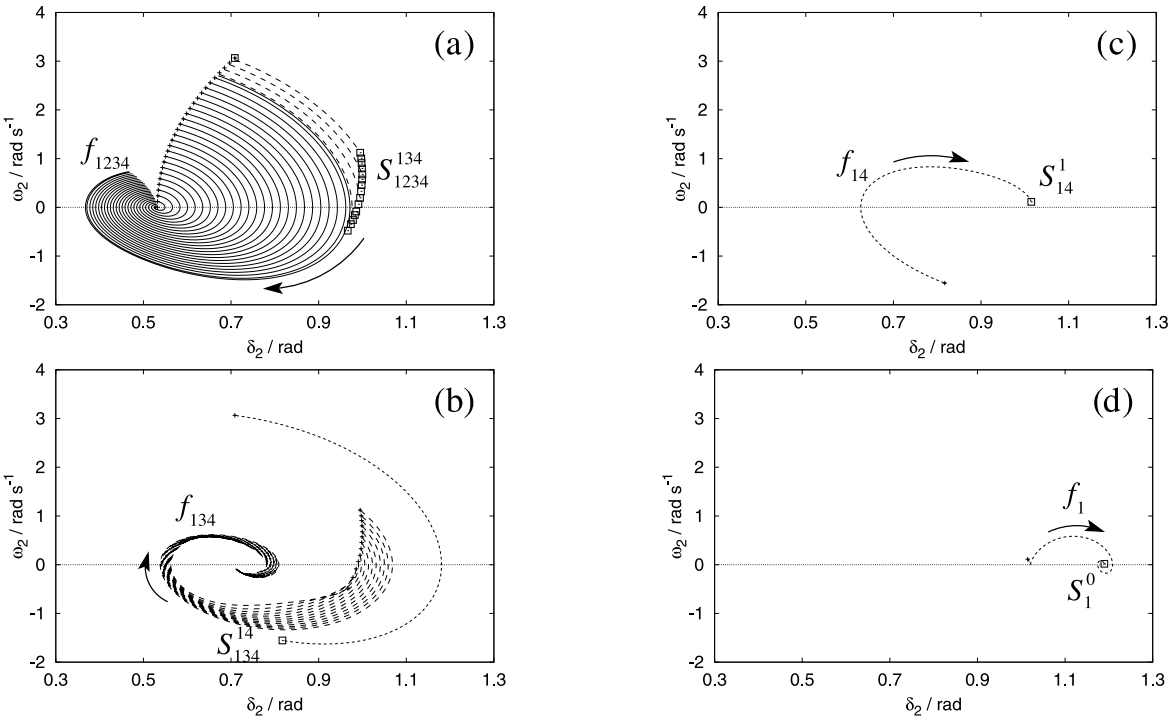

Fig. 5 Switching of flows governing the cascading outage in Fig. 4. f_α denotes the flow described by the classical model (1) indexed by α, and S^β_α the switching points at which the system's state is transferred from f_α to f_β. (a) f_{1234}; (b) f_{134}; (c) f_{14}; and (d) f_1. Each flow is drawn with its projection onto $\delta_2 - \omega_2$ plane.

CB2 ($t = 0.112$ s) $\rightarrow$ CB3 (0.688 s) $\rightarrow$ CB4 (1.631 s) $\rightarrow$ CB1 (3.133 s). The lines CB1–CB4 do not exist in the system model, and finally all the machines lose synchronism with the infinite bus. This propagation of outages reproduced is consistent with the data in Sect. 2. The occurrence of propagation is dependent on the fault duration t_c, which is analyzed in the next subsection. On the other hand, the numerical swings for rotor speed deviation ω_i in Fig. 4 are at most 3 rad/s $\approx$ 0.5 Hz $\times 2\pi$ and are not consistent with the data. This is because the data in Fig. 2 is measured at the large machine G5, and the places where it is measured in Fig. 1 are different from machines G1–G4 in Fig. 2.

4.2 Dynamical Studies

This subsection investigates the relationship between cascading outage and switching of flows. Thereby it is shown that the internal dynamics of protection operation play an important role in the cascading outage.

4.2.1 Switching of Flows Produces the Cascading Outage

Sequential portraits of the flow described by the classical model (1) are presented. Since the flows are defined on the atlas V with high dimensions, it is hard to visualize all the flow components. This subsection hence focuses on the flow that is obtained by varying the fault duration t_c in a given range $[0\,\mathrm{s}, T]$. T corresponds to the maximum duration.

Figure 5 shows trajectories of the hybrid dynamical system for $T = 0.112$ s. The trajectories are obtained by numerical integration of the classical model (1) for several values of t_c in $[0\,\mathrm{s}, T]$, and they are projected onto $\delta_2 - \omega_2$ plane. The right arc starting from $(\delta_2, \omega_2) \approx (0.52, 0)$, denoted by the mark '+,' shows the starting points of trajectories on flow f_{1234}. f_α denotes the flow described by the classical model (1) indexed by α. S^β_α, denoted by the mark '□,' shows the set of switching points at which the system's state is transferred from f_α to f_β. The trajectories, denoted by the *solid* lines in Fig. 5, contain no switching of flows and converge to a stable equilibrium point on f_{1234}. On the other hand, the trajectories, denoted by the *dotted* lines in Fig. 5, contain at least one switching of flows. After the system's state is transferred from f_{1234} to f_{134}, most of the trajectories converge to a stable equilibrium point on f_{134}. Here there is one trajectory in Fig. 5 for which the system's state is further transferred from f_{134}, to f_{14}, and to f_1. The sequence of switching points is $S^{134}_{1234} \rightarrow S^{14}_{134} \rightarrow S^{1}_{14} \rightarrow S^{0}_{1}$. The trajectory finally diverges on flow f_0 and corresponds to the cascading outage in Fig. 4.

The set of switching points S^{123}_{1234} is decomposed into two disconnected parts. Figure 6 shows time responses of internal states x_{12} of overcurrent relay and x_{22} of circuit breaker. The fault duration t_c is for (a) 0.086 s, (b) 0.09825 s, (c) 0.105 s, and (d) 0.112 s. The difference of each of (a)–(c) is based on the behavior of internal states x_{12} and x_{22} after the onset of fault clearing, $t = t_c$. In (a), x_{12} of overcur-

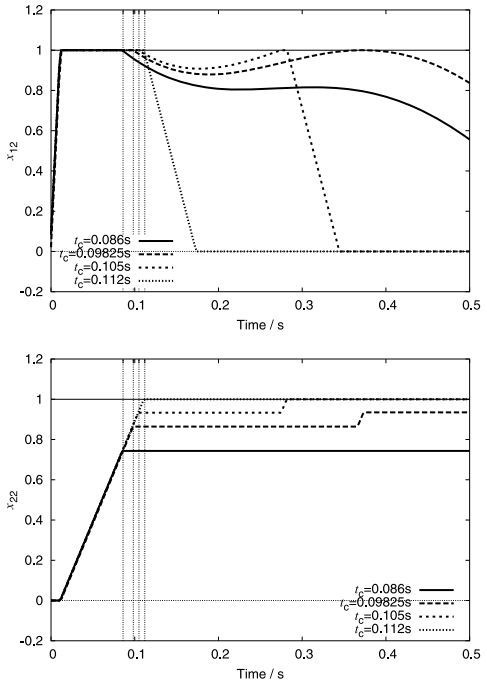

Fig. 6 Time responses of internal states x_{12} of the overcurrent relay and x_{22} of the circuit breaker of line CB2: (a) 0.086 s, (b) 0.09825 s, (c) 0.105 s, and (d) 0.112 s.

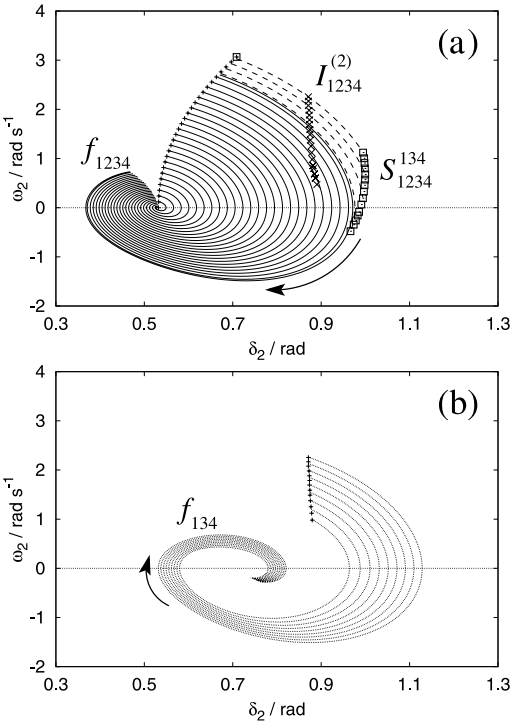

Fig. 7 Effect of internal dynamics in protection operation on the cascading outage in Fig. 4. (a) shows the flow f_{1234} on which the points $I^{(2)}_{1234}$ satisfying $I_2(\delta_1, \ldots, \delta_5) = I_{\mathrm{TAP}}$ are plotted. The flow itself is identical to that in Fig. 5(a). (b) shows trajectories in the case that the switching of flows from f_{1234} to f_{134} occurs on $I^{(2)}_{1234}$.

rent relay does not reach the threshold value $x_{12} = 1$. In (b), x_{12} reaches the threshold value $x_{12} = 1$ after $t = t_c$ and, however, x_{22} of circuit breaker does not reach the threshold value $x_{22} = 1$. In (c), x_{12} reaches 1 after $t = t_c$, and x_{22} also reaches 1. That is, these corresponding trajectories stay on f_{1234} in (a) and (b) infinite period and in (c) a finite period. On the other hand, the difference between (d) and each of (a)–(c) is based on the behavior of x_{22} before the onset of fault clearing. In (a)–(c), x_{22} does not reach its threshold before $t = t_c$. (d) corresponds to the case in Fig. 4 and indicates that x_{12} reaches 1 at $t = t_c$. This implies that in Figs. 5 and 6(d), the system's state at $t = t_c$ is immediately transitioned from f_{1234} to f_{123}. The difference between the onsets of switching results in the disconnection of S^{123}_{1234}.

From these numerical results, it is said that the cascading outage in Fig. 4 is produced as a result of the interplay between the flows describing swing dynamics of synchronous machines and their switching depending on the control schemes of protection operation.

4.2.2 Relay Internal Dynamics are Needed for the Cascading Outage

The control schemes of protection operation used here include internal dynamics, in other words, dynamic control laws described by Eqs. (3) and (5) with discrete outputs. The existence of internal dynamics is different from mathematical models of distance relays [28]–[30]. Next we consider the effect of internal dynamics in protection operation on the cascading outage in Fig. 4.

Figure 7(a) shows the flow f_{1234} on which the points $I^{(2)}_{1234}$ satisfying $I_2(\delta_1, \ldots, \delta_5) = I_{\mathrm{TAP}}$ are plotted with the mark '×.' The flow itself is identical to that in Fig. 5(a). The gap between $I^{(2)}_{1234}$ and S^{134}_{1234} along trajectories is caused by the internal dynamics. The main aim of the present analysis is to investigate whether the gap is needed for the cascading outage in Fig. 4. Figure 7(b) shows trajectories in the case that the switching of flows from f_{1234} to f_{134} occurs on $I^{(2)}_{1234}$. The trajectories converge to a stable equilibrium point on f_{134} and do not therefore show any cascading outage like that in Fig. 4. This fact indicates that the internal dynamics of protection operation are needed for the cascading outage in Fig. 4.

4.2.3 The Relay Parameter I_{TAP} Affects the Cascading Outage

The control schemes of protection operation have several parameters which are available as design and control objects. For modeling, it is necessary to estimate whether the cascading outage is observed for wide range of the parameters, in other words, whether it is robust to the change of parameters. Here we vary the parameter I_{TAP} of the threshold value in overcurrent relays, because it directly affects the switching mechanisms of flows as noted below.

Figure 8 shows the flow f_{1234} with (a) $I_{\mathrm{TAP}} = 1.00$ and (b) $I_{\mathrm{TAP}} = 1.05$. The flow with $I_{\mathrm{TAP}} = 1.03$ is shown in

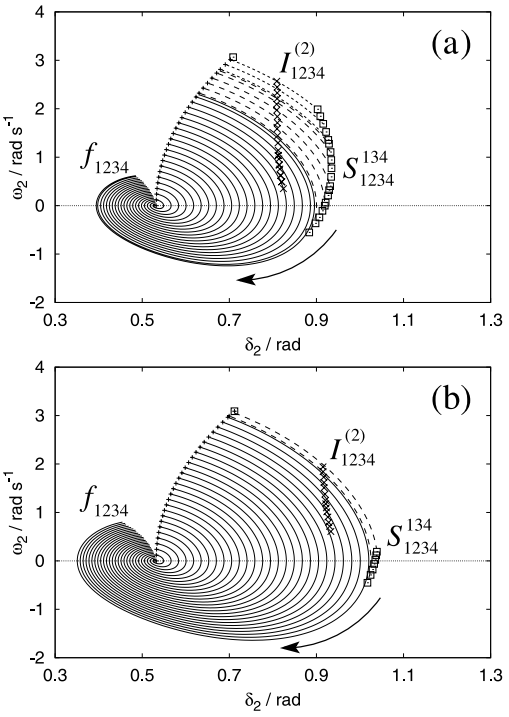

Fig. 8 Effect of the parameter I_{TAP} in overcurrent relays on the cascading outage in Fig. 4: (a) $I_{\mathrm{TAP}} = 1.00$ and (b) $I_{\mathrm{TAP}} = 1.05$. Each flow is drown with its projection onto $\delta_2 - \omega_2$ plane.

Fig. 5. The parameter change of I_{TAP} affects the position of $I^{(2)}_{1234}$ directly and that of S^{123}_{1234} indirectly. The flow itself is almost invariant although the internal dynamics depend on I_{TAP}. These figures show trajectories that contain the switching of flows from f_{1234} to f_{134}. This implies that the occurrence of outages similar to that in Fig. 4 persists against the change of the parameter I_{TAP}. Moreover, the area covered by the trajectories which include at least one switching decreases as I_{TAP} increases. This implies that the cascading outage can be avoided by appropriate tuning of relays such as adaptive relays [31].

From these numerical results, it is clear that the cascading outage scenario in Fig. 4 is affected by the switching rules of protection operation.

5. Summary and Remarks

We developed and analyzed a hybrid dynamical system as a mathematical model of cascading outage in a power system. The developed model consists of a family of flows describing swing dynamics of synchronous machines and their switching rules describing protection operation. This paper referred to data on a cascading outage in the September 2003 blackout in Italy and provided the hybrid dynamical system H by which propagation of outages reproduced was consistent with the data. The analysis of hybrid dynamical system in Sect. 4 indicates that switching of flows produces the cascading outage, and thus the protection operation with internal dynamics plays an important role in the cascading outage. The contribution here is the dynamical analysis of the cascading outage in a real power system from a viewpoint of hybrid dynamical systems. We close this paper with a few remarks of related and future work.

Modeling of power system dynamics via hybrid dynamical systems is not a new approach. A hybrid automaton is used in [10], [18] for modeling of power systems which considers transformer tap positions and relay internal states. A hybrid input/output automaton is adopted in [19] for an analysis of power transmission system. Previous work makes it possible to formulate hybrid dynamics of power systems. A hybrid dynamical system was used in [13] for modeling cascading failures of networked systems. The difference between the model in [13] and the developed hybrid model is that the hybrid model can explicitly consider discontinuous protection control to cause the cascading outage. This makes it clear that the cascading outage is produced by the switching of flows based on the protection mechanism.

Many research topics may follow the present study on cascading outages in power systems. We have two main goals: to derive minimal models of cascading outages that enable reproduction of their real data and prediction of their occurrence, and to use the model for designing controllers or operation algorithms that reduce cascading outages. For modeling goal, since real cascading outages are complicated as mentioned in Sect. 2, the developed model here is not enough to reproduce entire dynamics of the real outage. It is observed in real outages that voltage decrease induces undesirable actions of protection and can become a trigger of cascading outages. Detailed models with voltage dynamics are hence needed and will enable reproduction of the entire dynamics. For design goal, it is inevitable to clarify the benefit of mathematical formulation using the hybrid dynamical system. This paper cannot indicate the effectiveness of hybrid system representation H in comparison with conventional models. This point becomes significant for characterizing the relationship between performance of controllers based on the hybrid model and conventional ones.

Acknowledgment

We thank Dr. Yueheng Lan (University of California, Santa Barbara) for his careful reading of the manuscript.

References

[1] P. Fairley, "The unruly power grid," IEEE Spectr., vol.41, no.8, pp.22–27, Aug. 2004.
[2] C.W. Gellings and K.E. Yeager, "Transforming the electric infrastructure," Physics Today, vol.57, no.12, pp.45–51, Dec. 2004.
[3] I. Dobson, B.A. Carreras, V.E. Lynch, and D.E. Newman, "Complex systems analysis of series of blackouts: Cascading failure, critical points, and self-organization," CHAOS, vol.17, no.2, p.02610, June 2007.
[4] G. Andersson, P. Donalek, R. Farmer, N. Hatziargyriou, I. Kamwa, P. Kundur, N. Martins, J. Paserba, P. Pourbeik, J. Sanchez-Gasca, R. Schulz, A. Stankovic, C. Taylor, and V. Vittal, "Causes of the 2003 major grid blackouts in North America and Europe, and recommended means to improve system dynamic performance," IEEE

Trans. Power Syst., vol.20, no.4, pp.1922–1928, Nov. 2005.
[5] E.W. Kimbark, Power System Stability, John Wiley & Sons, New York, 1947.
[6] H.D. Chiang, "Power system stability," in Wiley Encyclopedia of Electrical and Electronics Engineering, ed. J.G. Webster, pp.105–137, John Wiley & Sons, New York, March 1999.
[7] S. Corsi and C. Sabelli, "General blackout in Italy Sunday September 28, 2003, h. 03:28:00," Proc. IEEE PES General Meeting, pp.1691–1702, Denver, USA, June 2004.
[8] W.H. Esselman, D.J. Sobajic, and J. Maulbetsch, "Hybrid discrete and continuous control for power systems," Discrete Event Dynamic Systems: Theory and Applications, vol.9, pp.297–318, 1999.
[9] L.H. Fink, "Discrete events in power systems," Discrete Event Dynamic Systems: Theory and Applications, vol.9, pp.319–330, 1999.
[10] I.A. Hiskens and M.A. Pai, "Hybrid systems view of power system modeling," Proc. IEEE International Symposium on Circuits and Systems, pp.228–231, Geneva, Switzerland, May 2000.
[11] R. Kinney, P. Crucitti, R. Albert, and V. Latora, "Modeling cascading failures in the North American power grid," European Physical J. B, vol.46, pp.101–107, 2005.
[12] P.A. Parrilo, S. Lall, F. Paganini, G.C. Verghese, B.C. Lesieutre, and J.E. Marsden, "Model reduction for analysis of cascading failures in power systems," Proc. American Control Conference, pp.4208–4212, San Diego, June 1999.
[13] C.L. DeMarco, "A phase transition model for cascading network failure," IEEE Control Syst. Mag., vol.21, no.6, pp.40–51, Dec. 2001.
[14] A. Back, J. Guckenheimer, and M. Myers, "A dynamical simulation facility for hybrid systems," in Hybrid Systems, ed. R.L. Grossman, A.P. Ravn, and H. Rischel, Lecture Notes in Computer Science 736, pp.255–267, Springer-Verlag, 1993.
[15] S.D. Johnson, "Simple hybrid systems," Int. J. Bifurcation Chaos Appl. Sci. Eng., vol.4, no.6, pp.1655–1665, June 1994.
[16] J. Guckenheimer and S. Johnson, "Planer hybrid systems," in Hybrid Systems II, ed. P. Antsaklis, A. Nerode, W. Kohn, and S. Sastry, Lecture Notes in Computer Science 999, pp.202–225, Springer-Verlag, 1995.
[17] T.A. Henzinger, "The theory of hybrid automata," Proc. 11th Annual IEEE Symposium on Logic in Computer Science, pp.278–292, 1996.
[18] I.A. Hiskens, "Power system modeling for inverse problems," IEEE Trans. Circuits Syst. I, Fundam. Theory Appl., vol.51, no.3, pp.539–551, March 2004.
[19] G.K. Fourlas, K.J. Kyriakopoulos, and C.D. Vournas, "Hybrid systems modeling for power systems," IEEE Circuits Syst. Mag., vol.4, no.3, pp.16–23, Third Quarter 2004.
[20] T. Hikihara, "Application of hybrid system theory to power system analysis (I)," Annual Meeting Record IEE Japan, p.187, March 2005.
[21] Y. Susuki, H. Ebina, and T. Hikihara, "Application of hybrid system theory to power system stability analysis," Proc. 2005 International Symposium on Nonlinear Theory and its Applications, pp.202–205, Bruge, Belgium, Oct. 2005.
[22] Y. Susuki, Y. Takatsuji, and T. Hikihara, "Hybrid model for cascading transient dynamics in power networks: A numerical study on five areas system," Proc. 51th Annual Conference of the Institutes of Systems, Control and Information Engineers (ISCIE), pp.331–332, Kyoto, Japan, May 2007.
[23] Y. Susuki, Y. Takatsuji, and T. Hikihara, "A hybrid model of cascading transient dynamics in multi-area power network," IEICE Technical Report, NLP2007-37, 2007.
[24] H.D. Chiang, C.C. Chu, and G. Cauley, "Direct stability analysis of electric power systems using energy functions: Theory, applications, and perspective," Proc. IEEE, vol.83, no.11, pp.1497–1529, Nov. 1995.
[25] M.A. Pai, Energy Function Analysis for Power System Stability, Kluwer Academic Pub., 1989.
[26] L.G. Perez, A.J. Flechsig, and V. Venkatasubramanian, "Modeling the protective system for power system dynamic analysis," IEEE Trans. Power Syst., vol.9, no.4, pp.1963–1973, Nov. 1994.
[27] I.M. Mitchell, "Comparing forward and backward reachability as tools for safety analysis," in Hybrid Systems: Computation and Control, ed. A. Bemporad, A. Bicchi, and G. Buttazzo, Lecture Notes in Computer Science 4416, pp.428–443, Springer-Verlag, 2007.
[28] C. Singh and I. Hiskens, "Direct assessment of protection operation and nonviable transients," IEEE Trans. Power Syst., vol.16, no.3, pp.427–434, Aug. 2001.
[29] V. Donde and I. Hiskens, "Dynamic performance assessment: Grazing and related phenomena," IEEE Trans. Power Syst., vol.20, no.4, pp.1967–1975, Nov. 2005.
[30] T. Sakiyama, T. Uemura, T. Ochi, T. Hikihara, Y. Susuki, and H. Ebina, "Application of hybrid system theory to power system analysis (IV)," Annual Meeting Record I.E.E. Japan, pp.269–270, 2006.
[31] S.H. Horowitz and A.G. Phadke, "Boosting immunity to blackouts," IEEE Power & Energy Magazine, vol.1, no.5, pp.47–53, Feb. 2003.

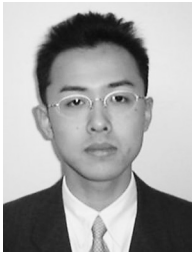

Yoshihiko Susuki received Ph.D. degree from Kyoto University in 2005. Since 2005 he has been with Department of Electrical Engineering at Kyoto University, where he is currently an Assistant Professor. He was a visiting scholar at Cornell University in 2003 and has been a visiting researcher at University of California, Santa Barbara since 2008. His research interests are in nonlinear dynamics, power system engineering, and control engineering. He is a regular member of the IEEE, APS, IEE Japan, and ISCIE.

Yu Takatsuji received B.E. degree from Kyoto University in 2007. He is currently working on power systems and hybrid systems in Graduate School of Engineering at Kyoto University.

Takashi Hikihara received Ph.D. degree from Kyoto University in 1990. Since 1997 he has been with Department of Electrical Engineering at Kyoto University, where he is currently a Professor. His research interests are in nonlinear science, nano elerctro-mechanical systems, and power engineering. He is currently an associate editor of European Journal of Control. He is a regular member of the IEEE, IET, APS, SIAM, IEE Japan, and ISCIE.